

Neuroinformatic tool to study high dimensional dynamics with distributed delays in Neural Mass Models

González Mitjans A.^{1,2,3,*}, Paz Linares D.^{1,2,4*}, Areces Gonzalez A.^{1,2,5}, Li M.^{1,2}, Wang Y.^{1,2}, Bringas-Vega M.L.^{1,2} and Valdés-Sosa P.A.^{1,2,4}

1. The Clinical Hospital of Chengdu Brain Science Institute, MOE Key Lab for Neuroinformation, University of Electronic Science and Technology of China, Sichuan, Chengdu, China, No. 2006, Xiyuan Ave., West Hi-Tech Zone, Chengdu, 611731, China

2. School of Life Science and Technology, Center for Information in Medicine, University of electronic Science and technology of China, Chengdu, China

3. Department of Mathematics, University of Havana, Havana, Cuba

4. Department of Neuroinformatic, Cuban Neuroscience Center, Havana, Cuba

5. Department of Informatics, University of Pinar del Rio, Pinar del Rio, Cuba

* Contributed equally

Abstract: Several of the theoretical bases have arisen from the examination of dynamic systems, using Neural Mass Models (NMMs). Due to the largescale brain dynamics of NMMs and the difficulty of studying nonlinear systems, the local linearization approach to discretize the state equation was used via an algebraic formulation, as it intervenes favorably in the speed and efficiency of numerical integration. To study the space-time organization of the brain and generate more complex dynamics, three structural levels (cortical unit, population and system) at the mesoscopic level were defined and assumed, in which a new representation for conduction delays given by distributed delays was established. We provide a distributed time-delay NMM, which can simulate several types of EEG activities since kinetics information was considered at three levels of complexity. Results obtained in this analysis provide additional theoretical foundations and indicate specific characteristics for understanding neurodynamic.

Keywords: Neural Mass Model, time-delay, connectivity matrix, brain dynamics, local linearization method.

1 Introduction

One of the factors to consider in neuronal modeling is the terms of experimental validation and the use of physical units to represent them. Because of this, many mathematical models have been developed to represent and describe the human brain, regardless of the level of abstraction and the assumptions that must be made for its formulation. A mathematical description of a neuron that predicts its dynamics and characterizes its properties, it is known as Neural Mass Model (NMM). Certain neuroscientists have considered this aspect and there are several software and packages such as GENESIS and NEURON, which are used to silico modeling of realistic neurons. Another remarkable software is the Blue Brain (BB) project, which aim to construct a biophysically detailed simulation of a cortical column on supercomputer with a high anatomical definition. They provide physical

description of the nervous system at the microscopic level^{[1]-[3]}.

On the other hand, there are others like The Virtual Brain (TVB), which is an available neuroinformatic platform to systematically study brain network models and neural fields mainly at mesoscopic level^{[4]-[7]}. It has various Neural Mass Models and Neural Field Models (NFM) implemented. To solve them they use Euler, Heun and 4th order Runge-Kutta methods for deterministic and stochastic schemes^{[8][9]}.

The main point in these tools is that detailed neuron descriptions require methods computationally expensive and without a fine time scale. In addition, the methods used for numerical calculations become explosive when initial values are in the phase space^{[10][11]} and also for simulations of stochastic systems^[12]. It is also known that, for small values of the integration step, the Markov chain is non-stationary for nonlinear functions, as is the case^{[13][14]}. Instead, this study obtain a stationary Markov chain by the Local Linearization Method (LLM), which provides unlike the others discretization methods, non-explosive discrete time dynamical systems^[10].

Another important aspect is the criterion followed to treat time delays. Many research groups, including TVB, have ignored delays and deal with info propagation as being instantaneous, or just like a Dirac- δ distribution since are the easiest way to describe NMM and NFM. Here, it is a different way for transmission delays is suggested given by a distributed delay. It was proved that delayed activity plays a crucial role in brain network dynamics and with this type of delays better system stability was achieved.

2 Model Description

2.1 Neural Mass

The brain is made up of billions of nerve cells, called neurons, grouped on different brain regions. From the neuronal level is possible to access to cortical structures and to the whole brain, which leads the

opportunity to study the dynamic behavior of the brain and the responses of the organism to different stimulus. Neurons (or neural masses) convert information obtained from stimuli in electrical pulses known as spikes, that is why the polarity of the cell is relevant.

The brain is divided into several groups of cells depending on their functionality. Think about these characteristics, the electrical properties of each neuron can be identified as three of its main components: dendrites, somas (or body of cells) and axons. There are two kinds of axons in neurons, with Myelin or unmyelinated^{[15][16]}. Then, the time that a neuron takes to transfer the information processed internally will depend on the intrinsic characteristics of its components, which being a relevant feature for the establishment of interneuron connectivity and is known as time-delays^{[17]-[19]}. This theory was perfectly exposed by Hodgkin and Huxley^[20].

Each neural mass or layer has as an average membrane potential, which constitutes the consequence of different inputs to the system. These inputs represent the average pulse density or firing rate and average pulse density, those are transformed through two important processes postsynaptic potential (PSP) function and the potential-to-rate function, respectively. The processes exposed above may be more complex in dependence on the number of neurons assumed in a cortical column. A cortical column (or cortical unit) is composed of thousands of neurons in synaptic contact with the same orientation, identical physiological properties and similar receptive fields^[21]. Cortical columns, while not the basic structure, make up the simplest level of study in NMMs, which has been examined by many researchers of the subject. The number of neural masses considered for scientists depends on the level of coarse graining they want to assume^{[22][23]}.

2.2 Neural Mass Model (NMM)

Models used to simulate the electrical activity of the brain with its intricate cortical structures are called Neural Mass Model. These models allow us to describe neural function at a mesoscopic level understanding the architecture of the neurons that generate electrophysiological data and quantify the mean firing rates through a mathematical formulation.

They are represented by a set of nonlinear differential equations and often have stochastic information. One of the oldest and most recognized models is the Hodgkin-Huxley model (1963), which is defined by a system of nonlinear ordinary differential equations

that reflect the propagation and emergence of action potentials. Electric potentials are a consequence of spiking neurons. The nerve cells that present this dynamic type are of greater importance in the biological study of neuron models.

Wilson and Cowan derived the NFM and recognized that to represent a good description of the neural network, realizing that the neural activities require macroscopic models. Through numerical solutions, they inspected the responses of a spatially localized neural population: excitatory and inhibitory neurons in the model employing two differential equations and found that the frequency of limit cycles as responses can guarantee the presence of several stability states in the system^{[24][25]}. NMMs are an essential aspect of the study of the Dynamic Causal Modeling (DCM) of technical electrophysiological. Estimate the parameters in the NMM by Bayesian inversion and analyze how well does the studied model corresponds to the observed data set is possible to do using DCM, which is a method to explore changes of the data trough time. A disadvantage of this causal modeling procedure is the input is treated as known, rather than stochastic, but even that, this theory has been used to investigate the steady state response^{[26][27]}.

Due to the need of more realistic representations of the brain as a whole, these models have a high dimensionality, which further complicate their treatment. Despite the efforts made to address the problem of high dimensionality, one of the main disadvantages of the tools already able is the method used to integrate numerically. That is why, it is one of the main objectives of the recent work.

2.3 Jansen and Rit-Zetterberg Neural Mass Model (JR-Zetterberg NMM). Single Cortical Unit Level

One of NMM most famous models is the one formulated by Jansen and Rit-Zetterberg. It is a lumped-parameter model and describes the interaction between excitatory and inhibitory neuron populations. Through parameters estimation, several waveforms and rhythms were obtained^[28]. This model generates similar responses to evoked potentials in simulation and real human data and also provides a set of values for the connectivity constants useful for simulating alpha activity as a response^{[29][30]}. How the connections are established influences on the responses and the nonlinear behavior of the system. The effects of the connections forward, backward and lateral are exposed. Besides, a longer duration of the transients evoked and exhibiting damped oscillations can be achieved. The main assumption of these works

took constant the extrinsic input, problem that was solved taking rhythmic inputs ^{[31][32]}. Others added a spike-rate adaption to the inhibitory neural population showing that most of the important behavior corresponds to the nonlinearity of the model. She relied on the analysis of linear systems for investigating changes of spectral responses according to its neurophysiological parameters ^[33].

JR-Zetterberg NMM models through three coupled nonlinear differential equations of the second order, which are transformed into a first-order system with six differential nonlinear equations. It performs a transformation of the action potential into the average of the postsynaptic potential, creating a delay in the synaptic transmission, which is essential to generate the oscillatory activity ^{[34]–[37]}.

A single unit is given, in this model, by the interaction between three neurons (or layers). The pyramidal (Pyr) cells, inhibitory (Inh) and stellate (Ste) layers are used to generate de average postsynaptic membrane potentials. “Cortical unit level” is considered for us as the most basic level of brain dynamics at the mesoscopic level. The state-space of the model and its internal dynamic between layers into a cortical unit are shown in Figure 1.

Pyramidal neurons in this model receive feedback from the stellate and inhibitory neurons. The input to a neural mass is transformed from an average pulse density to an average potential membrane, via postsynaptic potential function. Then, the output of the system will be a convolution of the input and the impulse response function. The impulse response function of the model (or the first-order kernel) is interpreted as the characteristic PSP elicited by a single incoming spike given by a Dirac- δ function as follows

$$h_l(t) = \begin{cases} H_l v_l t \exp\{-v_l t\} & t \geq 0 \\ 0 & t < 0 \end{cases} \quad (1)$$

The subscript l aludes to the different kind of layers, i.e., e_p : pyramidal excitatory, i : inhibitory and e_s stellate excitatory. H_l is the maximum amplitude of the PSP and v_l lump the characteristic decays transmission together, i.e., the time constant of the membrane for each layer $l = e_p, i, e_s$ involved in the model. τ_l is a lumped representation of the sum of the rate constants of passive membrane and other spatially distributed delays in the dendritic tree and satisfies that $v_l = 1/\tau_l$ ^[30].

The values of these parameters depend if the EPSP or the IPSP ^{[29][38][39]}. The maximum value of the EPSP is reached faster than the maximum of the IPSP, but the latter has a greater potential. There is also a static nonlinear sigmoid (the next potential-to rate) function, which transforms the average membrane potential of a neural population into an average firing rate ^{[28][40][41]}

$$S(v) = \frac{2e_0}{1 + \exp\{r(v_0 - v)\}} \quad (2)$$

where e_0 is the maximum average firing rate of the neural populations, v_0 is the PSP corresponding to e_0 and r is the slop of the sigmoid.

Here, instead of using Stochastic Differential Equations (SDE) relies on Random Delay Differential Equation (RDDE). This enables the solution of the integration of the neural masses step by step for more efficiency and at a reasonable time scale. It would appear if one uses a fine times scale (impossible in the other formulation) then what would happen is would be a very long time. On the contrary, if one uses a very fine time step, the events of the neuronal simulations become unconnected, since then inputs for any given neural mass are delayed and are fixed values the generation of the postsynaptic potentials and other states. The solution of this set of RDDE become uncoupled for each neural mass and they can be solved explicitly with a computational algebraic program.

The model is formulated as a set of first-order nonlinear random differential equations with the state

$$\text{vector } \mathbf{x}_l = \begin{bmatrix} y_l \\ x_l \end{bmatrix}.$$

The connections and the information about conduction delays was considered as follows

$$\begin{cases} \dot{y}_l(t) = x_l(t) \\ \dot{x}_l(t) = H_l v_l [\mu_l + \sigma_l \dot{w}_l(t) + S(z_l(t))] \\ - 2v_l x_l(t) - v_l^2 y_l(t) \end{cases} \quad (3)$$

The main variables are represented by y_l , the output of the PSP and its derivative \dot{x}_l , which were considered for each layer $l = e_p, i, e_s$. The random properties of the system are driven by a noise process $\mu_l + \sigma_l \dot{w}_l(t)$ as is showed in Figure 1. It only influences to the stellate neural mass, because of its shape, all system inputs are through it, then $\mu_l + \sigma_l \dot{w}_l(t) = 0$ when $l = e_p, i$. This random term represents the first derivative of a Brownian noise process with drift and infinitesimal

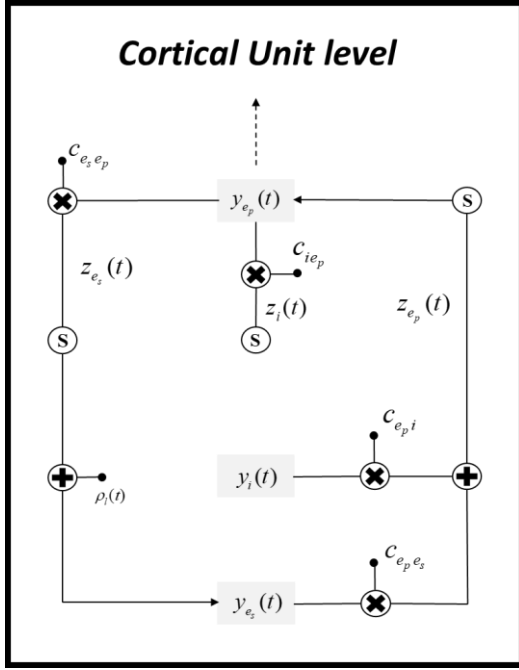


Figure 1: Jansen and Rit Neural Mass Model scheme for a single cortical unit. At this level, the interaction between excitatory and inhibitory layers is studied.

variance σ_{e_s} where $\dot{w}_{e_s}(t)$ is the first derivative of a unitary Brownian process. To an easier handling of random system input, it will be renamed it as $\rho_l(t)$.

This time, we deal with an algebraic interpretation of the JR-Zetterberg model, which make calculations easier and faster [42]. It provides a phase state analysis to study the behavior of two or more connected neural units. The Algebraic Differential Equation (ADE) [42]

$$z_l(t) = \mathbf{C}y_l(t) \quad (4)$$

Table 1: Standard values of Jansen and Rit NMM parameters

Parameter	Physiological interpretation	Value
H_l	Maximum amplitude of the PSP for excitatory and inhibitory neural masses respectively	3.25 mV, 22 mV
τ_l	Intrinsic lump parameters for excitatory and inhibitory neural masses respectively	10 ms, 50 ms
e_0	Maximum average firing rate of the neural populations	0.5 ms
v_0	The value of the potential	6 mV
r	Slope of the sigmoid at v_0	0.56 mV ⁻¹
c	Synaptic connections	135
$c_{e_p e_s}, c_{e_s e_p}$	Average number of synaptic contacts in the excitatory feedback loop	$c_{e_p e_s} = 108, c_{e_s e_p} = 135$
$c_{e_p i}, c_{i e_p}$	Average number of synaptic contacts in the slow feedback inhibitory loop	$c_{e_p i} = -33.75, c_{i e_p} = 33.75$

involves the variable $z_l(t)$, which is a linear combination of the PSP and the values of the synaptic connections between the neural mass $l = e_p, i, e_s$. Moreover, the output MEG/EEG signals are represented by the first component of this term (i.e., $z_l(t)$).

The matrix of coefficients $\mathbf{C} = \{c_{l_2 l_1}\}$, with zero diagonal entries, represent weights of the directed connections between two layers $l_2 \rightarrow l_1$. If $l_2 = l_1$, $l_1, l_2 \in l$, $l = e_p, i, e_s$ then $c_{l_2 l_1} = 0$ as are illustrated in the formulation (5). Its off-diagonal values are expressed as fractions of a constant $c = 135$, based on empirical knowledge of the EEG alpha-like activity [28][43]. The model connections scheme is displayed in Figure 1.

$$\begin{cases} c_{e_p i} = 0.25c & c_{e_p e_s} = 0.8c \\ c_{i e_p} = 0.25c & c_{e_s e_p} = c \end{cases} \quad (5)$$

Furthermore, the synaptic connectivity between neuron masses is positive except when it is from pyramidal to inhibitory cell (i.e., $l = i \rightarrow l = e_p$), in this case, it is negative.

$$\mathbf{C} = \begin{pmatrix} 0 & -33.75 & 108 \\ 33.75 & 0 & 0 \\ 135 & 0 & 0 \end{pmatrix} \quad (6)$$

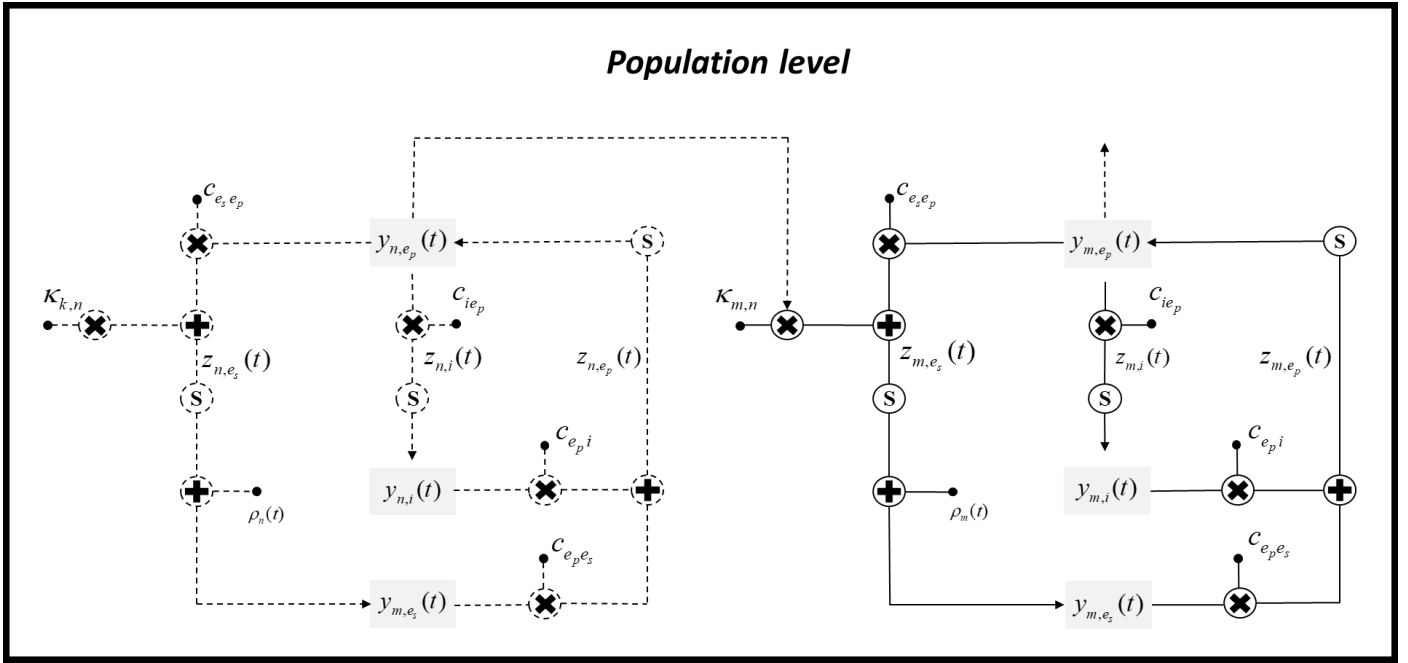


Figure 2: Population level is defined by the intercommunication of two or more cortical units. Here is schematized the linked between units n, m , where $n, m \in u$, $u = 1, \dots, Nu$.

Therefore, the ADE (4) could be expanded as

$$z_{l_1}(t) = \sum_{l_2=1}^3 c_{l_1 l_2} y_{l_2}(t - \tau_{l_1 l_2}) \quad (7)$$

where $\tau_{l_1 l_2}$ are the time lags for two connected layers $l_1, l_2 \in l$, $l = e_p, i, e_s$.

Once all the parameters of the JR-Zetterberg model are defined in Table 1 [28][41], they will represent the basis of this study. The brain is much more complex than we can imagine, so an extended study is necessary.

To describe interactions between cortical units was established the "population level" and with the inclusion of kinetics information the "system level" was defined to look at relations between populations. These two analyzes were displayed in the next subsection.

2.4 Model extension to complex levels: Population and System Levels

In this study, the interaction between two or several cortical units with similar characteristics was called population level and when have different rhythm belong to the system level. A schematic description of the interaction between two cortical units is shown in Figure 2. They conserve the original properties provided by the classical JR-Zetterberg model.

At these levels, the response function is like that of a single cortical column and the sigmoid function is also identical but the number of cortical units involved in the system is also measured are is described in the equations (8)-(10).

$$R_{ul}(t) = \begin{cases} H_{ul} v_{ul} t e^{-v_{ul} t} & t \geq 0 \\ 0 & t < 0 \end{cases} \quad (8)$$

$$\begin{cases} \dot{y}_{ul}(t) = x_{ul}(t) \\ \dot{x}_{ul}(t) = H_{ul} v_{ul} [\mu_{ul} + \sigma_{ul} \dot{w}_{ul}(t) + S(z_{ul}(t))] \\ - 2v_{ul} x_{ul}(t) - v_{ul}^2 y_{ul}(t) \end{cases} \quad (9)$$

$$z_{ul}(t) = \mathbf{K} y_{ul}(t) \quad (10)$$

Here, the variables and parameters were explained in the previously (see subsection 2.3), where $l = e_p, i, e_s$ indicates each layer (or neural mass). Now, $u = 1, \dots, Nu$ corresponds to cortical units and Nu is the total number of units involved in the model.

Here, the new approach is given by \mathbf{K} , which defines a connectivity tensor with connections and time-delay information between cortical units.

It is computed as

$$\mathbf{K} = \mathbf{K}_0 \cdot \mathbf{D} \quad (11)$$

Here, \mathbf{K}_0 is a matrix with the inter cortical unit connections and the connection strength tensor and \mathbf{D} contains weight-delay values given by an exponential distribution. A schematic description of the tensor connectivity formulation is displayed in Figure 3.

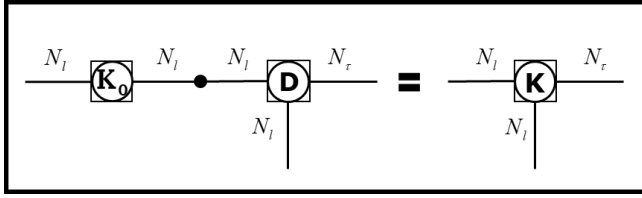


Figure 3: Tensor representation of connections and weight delays in NMMs, where N_l , N_r are the number of layers and time lags involved in the model.

Then, the output of the model at population and system levels may be calculated through the double sum of the connectivity tensor and the EPSP emitted from other units added to the MEG/EEG output z_l of the cortical unit level.

$$z_{u_1} = z_l + \sum_{u_2=1}^{Nu} \sum_{\tau=1}^{N\tau} \mathbf{K}_{u_1 u_2 \tau} y_{u_2 \tau} (t - \tau_{u_1 u_2}) \quad (12)$$

Here, $\tau_{u_1 u_2} \in [1, \dots, N\tau]$ refers to the time lags between two connected cortical units $u_1, u_2 \in u$, $u = 1, \dots, Nu$. The difference between population and system outcomes is that to obtain the system output is necessary to add neural kinetics features to the information obtained via population level, which allow the simulation of the relationship between different brain regions with different frequency bands^[30].

Since the NMM is formulated by a random nonlinear system, the analysis of this model is more complicated. That is why a linearization of the model was performed, using a method developed by Ozaki and colleagues.

3 Local linearization method (LLM)

The convection of the traditional JR-Zetterberg model to a system of algebraic differential equations was an important transformation to counteract out the problems of scale integration and facilitate the analysis of very large networks of neural masses with an efficient resolution^[42]. Here, the LLM of RDEs on the model was employed^[44]. This method for a single cortical unit will be exposed below. As is known, the manipulation of nonlinear systems is more complex, so it is widely important to find a linear equivalence.

Consider the state space of the model for a single cortical unit, given by equations (3) and (4). Let $\rho_l(t)$, $\mathbf{x}_l(t)$ be the random term and the state vector of the model respectively, where $l = e_p, i, e_s$ for each

$t \in [t_0, T]$ and f characterizes the k -dimensional RDE of the NMM as follows

$$\begin{aligned} d\mathbf{x}_l(t) &= f(\mathbf{x}_l(t), \rho_l(t)) dt \\ \mathbf{x}_l(t_0) &= \mathbf{x}_{l0} \end{aligned} \quad (13)$$

As this is a system of nonlinear stochastic differential equations, it can be solved numerically via LLM with a given step size for integration, i.e., $t_n = t_0 + nh$ and $n = 0, 1, \dots$. Then,

$$\mathbf{x}_l^{n+1} = \mathbf{x}_l^n + \mathbf{L} e^{J_f h} \mathbf{r} \quad (14)$$

where $\mathbf{r} = [0_{1 \times (k+1)}, 1]^T$, $\mathbf{L} = [\mathbf{I}_k, 0_{k \times 2}]$, with $k = 2$ and \mathbf{Jf} is defined by blocks as is shown in equation (1) in Appendix section.

Algebraic derivation was performed by MATLAB Symbolic Toolbox; a detailed procedure is given on a live script. The results of these operations are shown in equation (15), where H_l, v_l are the PSP parameters described in the previous section with $l = e_p, i, e_s$ and $dS(z_l(t))$ is the derivative of the sigmoid function.

$$\begin{aligned} \mathbf{Jf}_{x_l} &= \begin{pmatrix} 0 & 1 \\ -v_l^2 & -2v_l \end{pmatrix} \\ \mathbf{Jf}_{\rho_l} &= \begin{pmatrix} 0 & 0 \\ H_l v_l dS(z_l(t)) & H_l v_l \end{pmatrix} \end{aligned} \quad (15)$$

Furthermore, the full expression of \mathbf{Jf} is a (4×4) matrix, obtained after substitute the Jacobian matrices of f (See equation (2) in Appendix section).

In the next step of the LLM, after to apply the exponential matrix, a regrouping of terms was made, which simplifies and facilitates the compression and manipulation of the following numerical expression

$$\mathbf{x}_{l,t+h} = (\mathbf{I} + \mathbf{A}) \mathbf{x}_{l,t} + \mathbf{B} \mathbf{E}_{l,t} \quad (16)$$

where \mathbf{A} and \mathbf{B} are matrices with the PSP constants for each $l = 1, 2, 3$ neural mass, \mathbf{I} is the identity matrix and $\mathbf{E}_{l,t}$ contains the random inputs to the system and the sigmoidal function (See equation (3)-(5) in Appendix section)^[42].

To make the work easier, an auxiliary three-dimensional matrix of dimension $(3 \times 2 \times 4)$ was created to carry out the algebraic numerical integration, which contains the PSP integration factors

for each $l = e_p, i, e_s$. This new term grouping has an advantage, it allows you to create a multidimensional array (also interpreted as a tensor) that will not change.

A and **B** matrices are constants for each layer $l = e_p, i, e_s$ regardless of the level being analyzed, which favors numerical computations.

The same procedure was followed to analyze more complex dynamics, i.e., population and system levels. At system level, their dimension increase, containing the initial matrices **A** and **B** for each population (gamma, beta, alpha, theta and delta). While the arrays containing the PSP info do not change, the way the MEG/EEG output is generated changes depending on the level being analyzed, which influences the value of $\mathbf{E}_{l,t}$ or $\mathbf{E}_{u,t}$ according to the level studied. But it is necessary first to define how transmission delays will be assumed, compute $z_l(t)$ (or $z_u(t)$) and then $\mathbf{E}_{l,t}$ (or $\mathbf{E}_{u,t}$), without loss of generality.

4 Transmission delays analysis

4.1 New Interpretation for Weight-Delays

Consider a tensor $\mathbf{D}_{N_l N_i N_\tau}$, with weight-delays between neurons, where N_l , N_τ are the number of layers and time lags involved in the model.

Due the intrinsic transmission delays in a unit is small, was considered as a Dirac distribution, while for the time delays between two different units and populations, were simulated as an exponential distribution. To generate the center of the distribution, it was necessary to first select a frequency (in Hz) that would be present in the cortical unit and characterize the frequency of the population. The values of a lumped representation of the rate constants of the passive membrane and other spatially distributed delays in the dendritic tree (τ_l , $l = e_p, i, e_s$) to generate the different frequencies bands were empirically estimated [30]. Therefore, five populations will be created, each characterized by a different frequency band (delta, theta, alpha, beta, and gamma) and the neural dynamics between them will define the system level.

The excitatory layers are given by the Pyr ($l = e_p$) and the Ste ($l = e_s$) layers and the inhibitory, as its name implies by the Inh ($l = i$) layer. Then, it will be considered τ_e, τ_i for the excitatory and inhibitory layers, respectively. These parameters were obtained through a comparative and analogous estimation,

taking data from previous works, and extrapolating it to provide the estimation for the current research. The estimated values of lump parameters used to obtain oscillatory behavior are shown in Table 2.

Table 2: Estimation of the excitatory and inhibitory intrinsic lump parameters

Frequency bands	τ_e	τ_i
gamma (>30 Hz)	1 ms	4.8 ms
beta (12-30 Hz)	4.5 ms	10.7 ms
alpha (8-12 Hz)	10 ms	20 ms
theta (4-8 Hz)	15 ms	40.7 ms
delta (1-4 Hz)	20 ms	52 ms

There is a constant ratio for the values of both, excitatory and inhibitory layers, which was very useful to estimate the intrinsic lump parameters and it is formulated as

$$\frac{H_l}{\tau_l} = \begin{cases} 0.325 & \text{if } l = 1, 3 \\ 1.1 & \text{if } l = 2 \end{cases} \quad (17)$$

For the simulation at the unit and population level, it is only necessary to select one of the frequencies presented in Table 2, according to the interests of the researcher. While generating the dynamics at the system level it will be necessary to consider all the frequencies bands, showing the differences between populations with different frequencies and will make the simulation more realistic.

To compute a tensor with the weight-delay information **D**, were considered the center of the delay distribution τ_0 and the width of the delay distribution σ_0 , then

$$\mathbf{D} = \exp \left\{ - \left(\frac{t - \tau_0}{\sigma_0} \right)^2 \right\} \quad (18)$$

These parameters were obtained through the process to create synthetic directed connectivity and delays, which internally needs the frequency that will be used in the cortical unit and population simulations or a set of frequencies for the system level.

To generate the connectome was used as base the classic connectivity matrix estimated by Jansen and Rit. From this procedure the values of the parameters $\tau_0, \tau_{\max}, \sigma_0$ and \mathbf{K}_0 are obtained, which are the

center of the delay distribution, the maximum of the lag distribution, the width of the delay distribution and the information about the connection between the cortical units (or populations) involved. For the population analysis, the connections are defined from $u_1 \rightarrow u_2, u_2 \rightarrow u_1$, with $u_1, u_2 \in u, u = 1, \dots, Nu$ and for the system level, the connections are given two to two between the five populations generated by different frequencies. These results are used to compute the connectivity tensor \mathbf{K} which is widely important for generating the input to the system $z_{u_1}(t)$, with $u_1 \in u, u = 1, \dots, Nu$.

4.2 Influence of different time-delays on brain dynamics

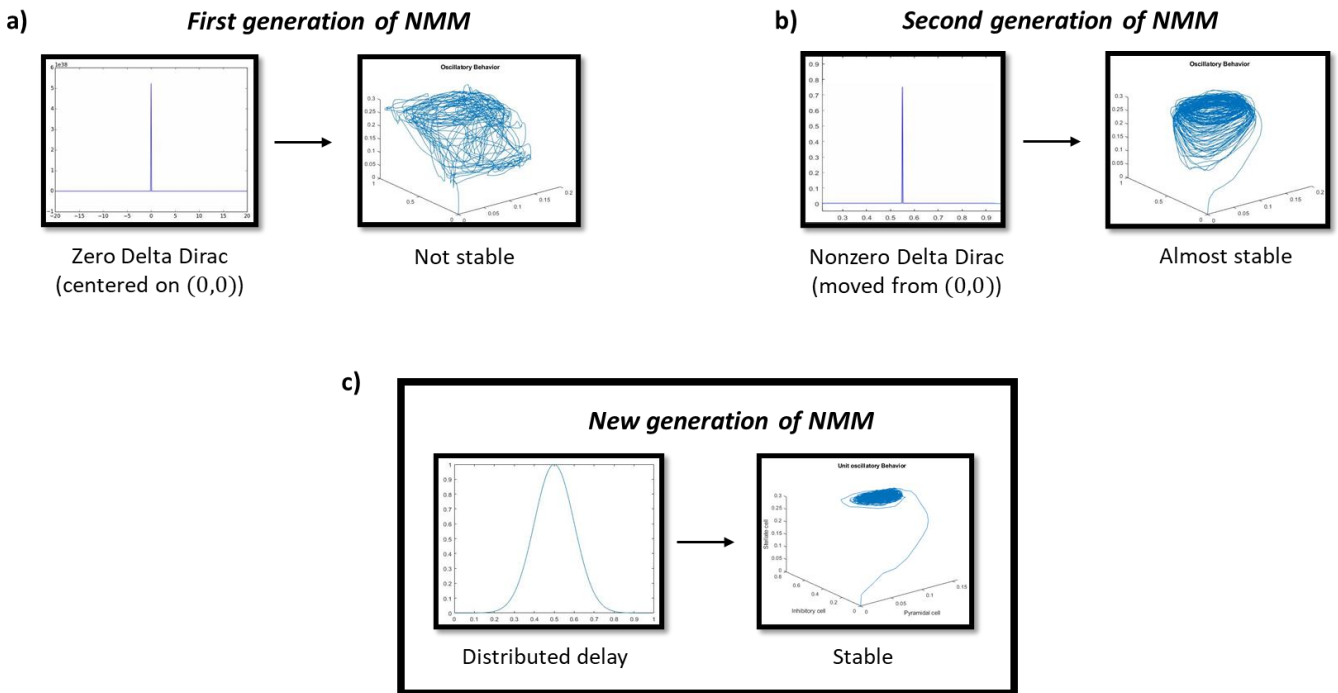
Scientific studies have assumed homogeneous time delays, sometimes they do not have it in consideration, or are represented as a Dirac - δ distribution. Several results in the literature show that each area in the brain may show differences in conduction delays produced by the variety of axonal characteristics depending on the diameter, speed and length of the axon. [4][24][31][42][45]-[49]. The consideration of delays in the frequency bands of the EEG, influences in the propagation of spikes over space. Sometimes have been used connectivity kernels to provide an explicit parameterization of conduction delays via the field

evident, and their effects may be important aspects of applications. Oscillatory behavior confirm also that they are particularly sensitive to delays, and for coupled multi-dimensional oscillators, time delays are known to cause amplitude and oscillation death [47][50]-[54].

In this work, due to the relevance of transmission delays, three different interpretations were examined and two of them were studied in previous papers. First, we test with a fixed value, which represent the “first generation of NMMs” via a Dirac- δ function centered at the origin and the “second generation of NMMs” given by a moved from the origin Dirac- δ distribution [9][35][55]-[57]. Some researchers have focused on finding a good approximation to represent the time delay suffered by the neural transmission of information [4][58][59]. Despite efforts of including delays, these models still had problems. The conduction-delays considered until now make the temporal dimension not well represented.

It can be written as a sum of two points connections, given for two different layers $l_1, l_2 \in l, l = e_p, i, e_s$ as follows

$$z_{l_1}(t) = \sum_{l_2=1}^3 c_{l_1 l_2} y_{l_2}(t - \tau_{l_1 l_2}) \quad (19)$$



model as an observation model [27]. Therefore, the influence of conduction delays in these models is

Figure 4: Graphic illustration of previously studied NMM conduction delays values and a new one was introduced. **a)** represents a Delta Dirac function centered on the origin as initial time delays considered into NMM, which yields to non-stable oscillatory behavior. **b)** contains time delays and oscillatory behavior of neural masses examined under a Delta Dirac distribution far from the origin. **c)** is the new distributed delay explored in this work and the related neural dynamics. Brain dynamics were found to be closely connected to the way used to interpret time-delays. A distributed delay provides a greater stability in NMM.

where $\tau_{1,2}$ represents the conduction delay estimated as a multiplication of the average path length between voxels (nodes), and conduction velocity is 10m/s [28][30][41][42].

As many of the natural phenomena have an exponential evolution over time, was explored how the JR-Zetterberg model behaves with this kind of distribution. We found the model is very sensitive to changes to transmission delays, which is reflected on the system stability. Therefore, the way in which the delays are represented is very important. As evidenced in Figure 3 the new interpretation for driving delays

implemented in this work provides greater stable oscillations for the NMM.

5 Results and Discussion

In the current work was simulated electroencephalography (EEG) data generated by a new formulation of the JR-Zetterberg NMM. Due to the existence of the time delay needed to propagate the actual signals among neurons, a new time-delay NMM and tools to study its dynamical behavior were developed rather than maintaining the tendency of previous researchers to employ a Dirac distribution. It was established as an exponential distribution,

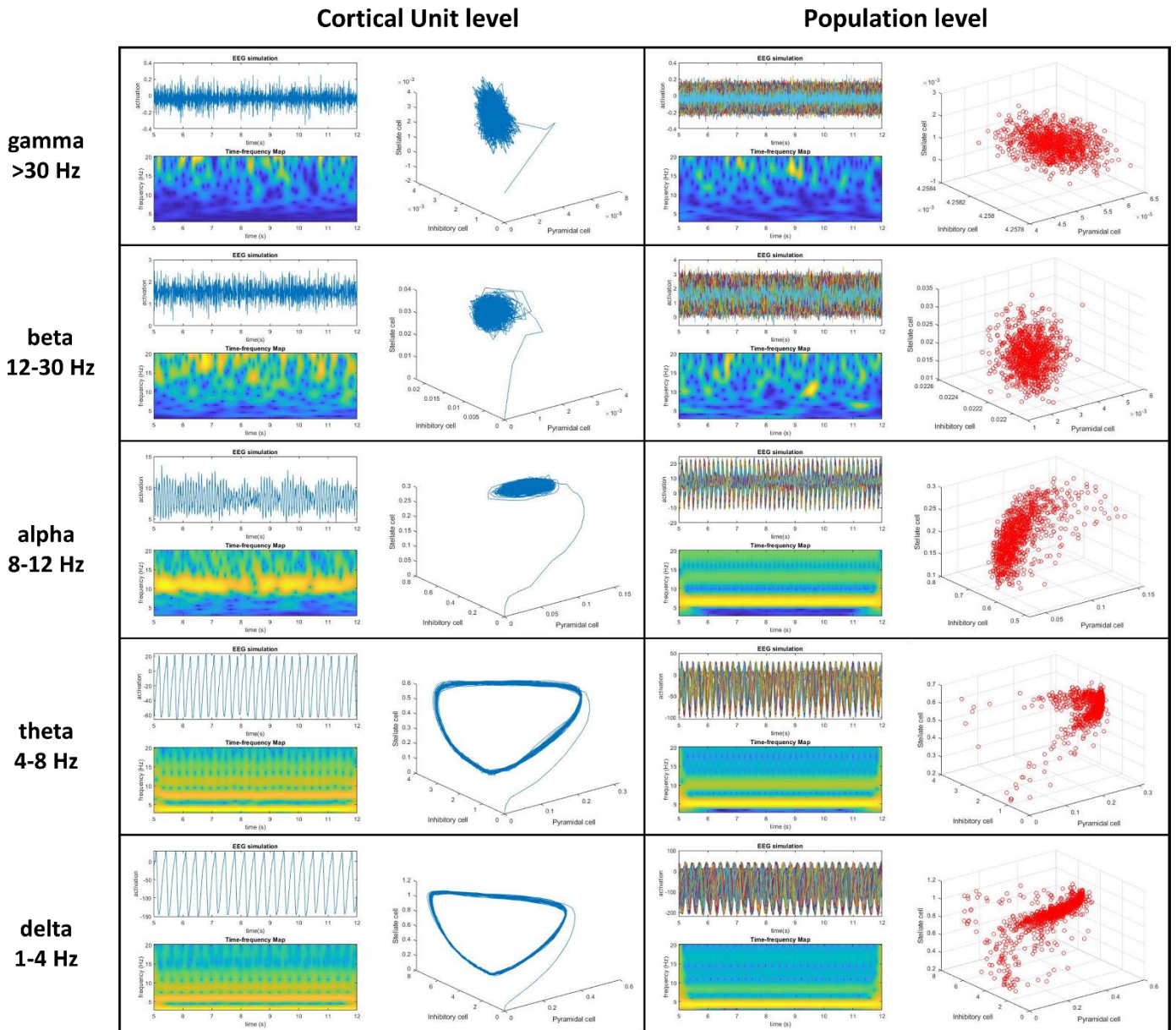


Figure 5: Brain simulation at cortical unit and population levels. Each row represents different frequency bands for the two simulated levels. The first column of each level contains an EEG simulated recording and a time-frequency map, while the second one describes the oscillatory behavior of neurons and units (1000) at unit and population levels, respectively. The assumptions show their validity, since brain activity is consistent at both levels compared to previous studies and the time-frequency description correspond to the real frequency values of the EEG bands. The oscillatory responses are stable for each frequency at both levels and as the frequency decreases the stability of the model increases, showing a limit cycle.

effectively simulating the conduction delays of the signals across the axon and its advantage was proven. Conduction delays and connections were combined on a clear tensor implementation, making the temporal dimension well represented.

The study of NMM in a single cortical unit was extended, developing a brain simulator at three levels, including kinetics information (gamma, beta, alpha, theta, delta) shown in Figure 6 and Figure 7. Through the simulated EEG recordings for each rhythm using the new form assumed to consider conduction delays, it was found that there is a greater similarity to the signals emitted during real EEG analysis and they are consistent with the values of these frequencies and their neural dynamics. The brain simulations reach a limit cycle behavior depend on decreasing the frequency. For larger cortical units (10000 units) stable simulations were obtained that could produce many types of EEG frequency spectra and stable behavior

was found also mixing units with different characteristic frequencies (See Figure 6).

These findings can indicate specific characteristics for each frequency bands, which coincide with the idea developed by Lopez da Silva about the importance of the oscillations emitted by lower frequencies to establish a functional bias in populations with a large number of neurons. It can also be of great relevance in obtaining specific response information in resting state and on neuronal sets interacting under a particular task.

The implementation of the computational tool developed to carry out these studies were fast and efficient despite the high dimensionality of the problem and the inclusion of kinetics information. This was made possible by an algebraic reformulation of the classic JR-Zetterberg model, which speeds up the speed of the program and makes calculations for

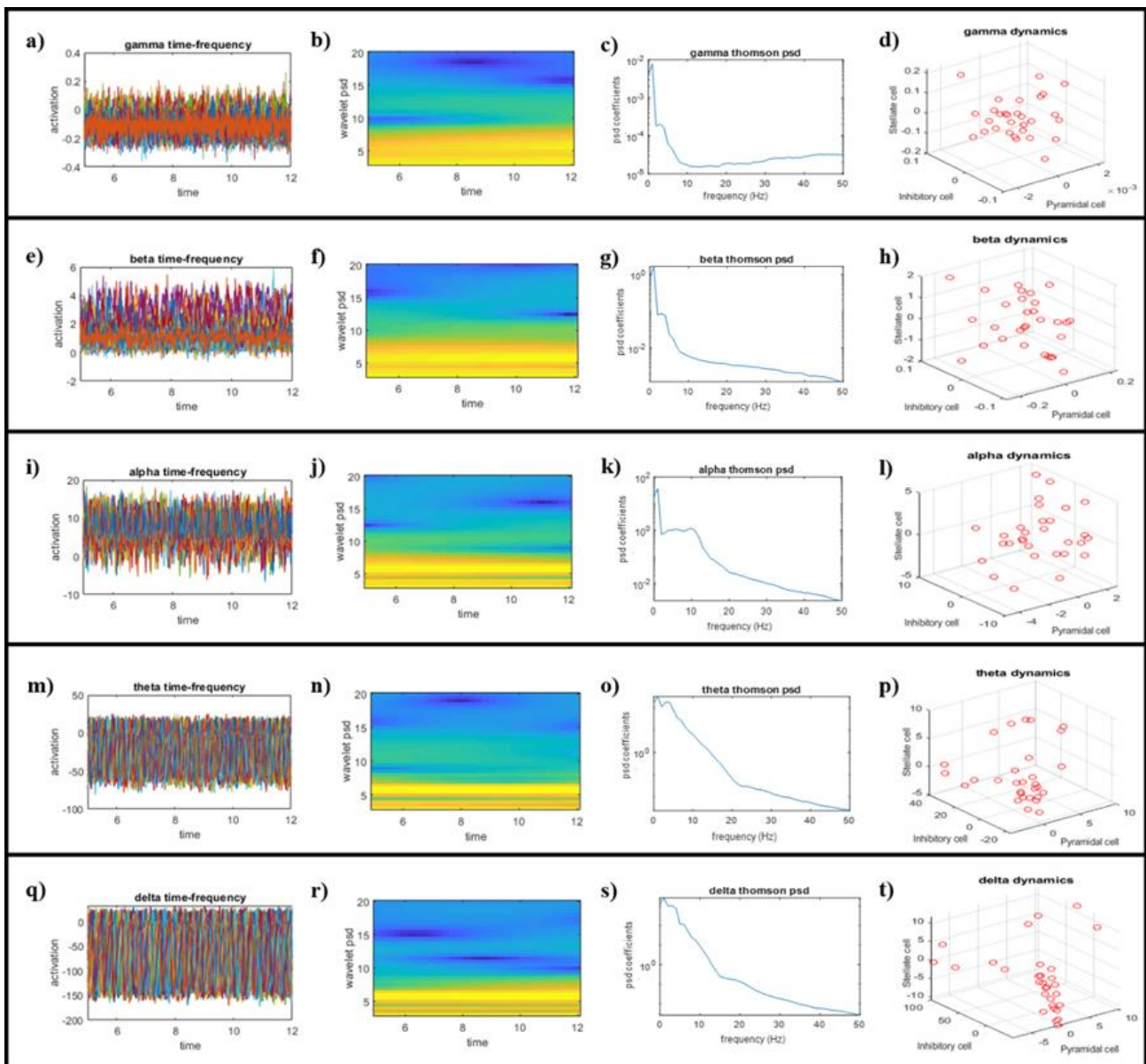


Figure 6: System level simulations. Stable behavior was found also mixing cortical units with different characteristic frequencies.

numerical integration easier. This is a very important aspect as many of the researchers in this field are using traditional methods to integrate numerically, such as Euler, Heun and Runge Kutta, which have a higher computational cost and become explosive when initial values are in the close to the phase space. The algebraic numerical integration was done in Live Script integrated into MATLAB as a tool to be disseminated.

6 Conclusions

A re-deduction of previous results was made, which had some errors, unifying the notation and many formulas were derived again looking for an algorithmic form that would optimize the calculation. Oscillatory activity occurs when there are interactions between excitatory and inhibitory neuron masses. With the new consideration of delays the temporal dimension was extended, representing the interaction between neurons through a connectivity tensor via specific connection weight and time delays. This new time-delay NMM can simulate several different types of EEG activities since kinetics information was considered, which influence on the oscillatory frequency. An expansion of the previous model was done, considering new structural levels (unit, population and system levels) and different types of human brain rhythms (from gamma to delta).

This research makes available a toolbox to move toward more realistic large-scale brain modeling. It allows a high-performance simulation of the neural dynamic behavior according to connectivity information. It enables fast and efficient implementation of those basic core of calculations, due the numerical integration was carried out via algebraic equations using LLM and integrates symbolic and numerical analysis to provide a new way of introducing delays into NMM.

References

- [1] M. A. Wilson, U. S. Bhalla, J. D. Uhley, et al. GENESIS: A System for Simulating Neural Networks [J]. *Advances in Neural Information Processing Systems 1 (NIPS 1988)*, 1989, 485–492.
- [2] J. M. Bower, D. Beeman, and M. Hucka. The GENESIS Simulation System California Institute of Technology Pasadena, CA 91125 University of Colorado Boulder, CO 80309 California Institute of Technology [J]. 2003, (January).
- [3] G. M. Shepherd. *Foundations of the neuron doctrine* [M]. 2015.
- [4] P. Ritter, M. Schirner, A. R. McIntosh, et al. The Virtual Brain Integrates Computational Modeling and Multimodal Neuroimaging [J]. *Brain Connectivity*, 2013, 3(2):121–145.
- [5] P. Sanzleon, S. A. Knock, M. M. Woodman, et al. The virtual brain: A simulator of primate brain network dynamics [J]. *Frontiers in Neuroinformatics*, 2013, 7(MAY).
- [6] M. Schirner, S. Rothmeier, V. K. Jirsa, et al. An automated pipeline for constructing personalized virtual brains from multimodal neuroimaging data [J]. *NeuroImage*, 2015, 117:343–357.
- [7] V. K. Jirsa, O. Sporns, M. Breakspear, et al. Towards the virtual brain : network modeling of the intact and the damaged brain [J]. 2010, 189–205.
- [8] P. Sanz-Leon, S. A. Knock, A. Spiegler, et al. Mathematical framework for large-scale brain network modeling in The Virtual Brain [J]. *NeuroImage*, 2015, 111:385–430.
- [9] A. Spiegler and V. Jirsa. Systematic approximations of neural fields through networks of neural masses in the virtual brain [J]. *NeuroImage*, 2013, 83:704–725.
- [10] T. Ozaki. *Nonlinear time series models and dynamical systems* [G]. 1985, 5:25–83.
- [11] R. Biscay, J. C. Jimenez, J. J. Riera, et al. Local linearization method for the numerical solution of stochastic differential equations [J]. *Annals of the Institute of Statistical Mathematics*, 1996, 48(4):631–644.
- [12] T. Howell. *Non Linear Time Series. A Dynamical System Approach* [M]. Oxford: Clarendon Press ; New York : Oxford University Press, 1990.
- [13] D. A. Jones and D. R. Cox. Nonlinear autoregressive processes [J]. *Proceedings of the Royal Society of London. A. Mathematical and Physical Sciences*, 1978, 360(1700):71–95.
- [14] P. Henrici. *Discrete variable methods in ordinary differential equations* [J]. 1962.
- [15] E. Luders, P. M. Thompson, and A. W. Toga. The development of the corpus callosum in the healthy human brain [J]. *Journal of Neuroscience*, 2010, 30(33):10985–10990.
- [16] D. K. Hartline. What is myelin? [J]. *Neuron Glia Biology*, 2008, 4(2):153–163.
- [17] M. W. Barnett and P. M. Larkman. The action potential [J]. *Practical neurology*, 2007, 7(3):192–197.
- [18] D. Junge. *Nerve and muscle excitation* [M]. 1992, (591.18 JUN).
- [19] H. Takagi. Roles of ion channels in EPSP integration at neuronal dendrites [J]. *Neuroscience research*, 2000, 37(3):167–171.

- [20] A. L. Hodgkin and A. F. Huxley. A quantitative description of membrane current and its application to conduction and excitation in nerve [J].*The Journal of physiology*, 1952, 117(4):500–544.
- [21] Z. Molnár. Cortical Columns [J].*Neural Circuit Development and Function in the Healthy and Diseased Brain*, 2013, 3:109–129.
- [22] T. D. Albright, T. M. Jessell, E. R. Kandel, et al. *Neural Science : A Century of Progress and the Mysteries that Remain* [J]. 2000, 100:1–55.
- [23] J. Lübke and D. Feldmeyer. Excitatory signal flow and connectivity in a cortical column: focus on barrel cortex [J].*Brain Structure and Function*, 2007, 212(1):3–17.
- [24] H. R. Wilson and J. D. Cowan. Excitatory and Inhibitory Interactions in Localized Populations of Model Neurons [J].*Biophysical Journal*, 1972, 12(1):1–24.
- [25] S. Coombes, P. Beim Graben, R. Potthast, et al. *Neural fields: Theory and applications* [J].*Neural Fields: Theory and Applications*, 2014, 9783642545(July):1–487.
- [26] R. J. Moran, K. E. Stephan, T. Seidenbecher, et al. Dynamic causal models of steady-state responses. [J].*NeuroImage*, 2009, 44(3):796–811.
- [27] D. A. Pinotsis, R. J. Moran, and K. J. Friston. Dynamic causal modeling with neural fields [J].*NeuroImage*, 2012, 59(2):1261–1274.
- [28] B. H. Jansen and V. G. Rit. Electroencephalogram and visual evoked potential generation in a mathematical model of coupled cortical columns. [J].*Biological cybernetics*, 1995, 73(4):357–366.
- [29] B. H. Jansen, G. Zouridakis, and M. E. Brandt. A neurophysiologically-based mathematical model of flash visual evoked potentials [J].*Biological Cybernetics*, 1993, 68(3):275–283.
- [30] O. David and K. J. Friston. A neural mass model for MEG/EEG: Coupling and neuronal dynamics [J].*NeuroImage*, 2003, 20(3):1743–1755.
- [31] O. David, L. Harrison, and K. J. Friston. Modelling event-related responses in the brain. [J].*NeuroImage*, 2005, 25(3):756–770.
- [32] A. Spiegler, T. R. Knösche, K. Schwab, et al. Modeling brain resonance phenomena using a neural mass model [J].*PLoS Computational Biology*, 2011, 7(12).
- [33] R. J. Moran, S. J. Kiebel, K. E. Stephan, et al. A neural mass model of spectral responses in electrophysiology [J].*NeuroImage*, 2007, 37(3):706–720.
- [34] F. H. Eeckman and W. J. Freeman. Asymmetric sigmoid non-linearity in the rat olfactory system. [J].*Brain research*, 1991, 557(1–2):13–21.
- [35] A. Spiegler, S. J. Kiebel, F. M. Atay, et al. Bifurcation analysis of neural mass models: Impact of extrinsic inputs and dendritic time constants [J].*NeuroImage*, 2010, 52(3):1041–1058.
- [36] J. Touboul, F. Wendling, P. Chauvel, et al. Neural mass activity, bifurcations, and epilepsy [J].*Neural Computation*, 2011, 23(12):3232–3286.
- [37] V. Svozilova, M. Mezl, V. Svozilova, et al. Modeling of the EEG signal [J]. 2016.
- [38] W. J. Freeman. Models of the dynamics of neural populations. [J].*Electroencephalography and clinical neurophysiology. Supplement*, 1978, (34):9–18.
- [39] F. Grimbert and O. Faugeras. Analysis of Jansen’s model of a single cortical column [J].*Current Biology*, 2006, 14(1):34.
- [40] H. Kwakernaak and M. Sebek. Polynomial J-spectral factorization [J].*IEEE Transactions on Automatic Control*, 1994, 39(2):315–328.
- [41] B. H. Jansen and V. G. Rit. A mathematical model of coupled cortical columns [J].*Biological Cybernetics*, 1995, 366:357–366.
- [42] P. A. Valdes-Sosa, J. M. Sanchez-Bornot, R. C. Sotero, et al. Model driven EEG/fMRI fusion of brain oscillations [J].*Human Brain Mapping*, 2009, 30(9):2701–2721.
- [43] K. W. Yau. Receptive fields, geometry and conduction block of sensory neurones in the central nervous system of the leech [J].*The Journal of physiology*, 1976, 263(3):513–538.
- [44] F. Carbonell, J. C. Jimenez, R. J. Biscay, et al. The local linearization method for numerical integration of random differential equations [J].*BIT Numerical Mathematics*, 2005, 45(1):1–14.
- [45] V. K. Jirsa and H. Haken. Field theory of electromagnetic brain activity [J].*Physical Review Letters*, 1996, 77(5):960–963.
- [46] P. L. Nunez. The brain wave equation: a model for the EEG [J].*Mathematical Biosciences*, 1974, 21(3–4):279–297.
- [47] P. Sanz-Leon, S. A. Knock, A. Spiegler, et al. Mathematical framework for large-scale brain network modeling in *The Virtual Brain* [J].*NeuroImage*, 2015, 111:385–430.
- [48] V. K. Jirsa and H. Haken. A derivation of a macroscopic field theory of the brain from the quasi-microscopic neural dynamics [J].*Physica D: Nonlinear Phenomena*, 1997, 99(4):503–526.
- [49] P. A. Robinson, C. J. Rennie, and D. L. Rowe. Dynamics of large-scale brain activity in normal arousal states and epileptic seizures [J].*Physical Review E*, 2002, 65(4):41924.
- [50] F. Grimbert and O. Faugeras. Analysis of

Jansen's model of a single cortical column [J].2006.

- [51] P. A. Valdes, J. C. Jimenez, J. Riera, et al. Nonlinear EEG analysis based on a neural mass model [J].1999, 424:415–424.
- [52] S. Geng, W. Zhou, X. Zhao, et al. Bifurcation and oscillation in a time-delay neural mass model [J].*Biological Cybernetics*, 2014, 108(6):747–756.
- [53] F. Grimbert and O. Faugeras. Bifurcation Analysis of Jansen's Neural Mass Model [J].*Neural Computation*, 2006, 18(12):3052–3068.
- [54] A. Koseska, E. Volkov, and J. Kurths. Oscillation quenching mechanisms: Amplitude vs. oscillation death [J].*Physics Reports*, 2013, 531(4):173–199.
- [55] W. J. Freeman and J. Walter. Mass action in the nervous system [J].2004.
- [56] O. Faugeras, J. Touboul, and B. Cessac. A constructive mean-field analysis of multi-population neural networks with random synaptic weights and stochastic inputs [J].*Frontiers in Computational Neuroscience*, 2009, 3(FEB):1–28.
- [57] R. Moran, D. A. Pinotsis, and K. Friston. Neural masses and fields in dynamic causal modelling [J].*Frontiers in Computational Neuroscience*, 2013, 7(APR 2013):1–12.
- [58] I. Bojak and D. T. J. Liley. Axonal velocity distributions in neural field equations [J].*PLoS Computational Biology*, 2010, 6(1).
- [59] K. J. Friston, L. Harrison, and W. Penny. Dynamic causal modelling [J].2003, 19:1273–1302.

7 Appendix

This section collects several equations and mathematical formulations of the LLM due to their length.

- Jacobian matrix for local linearization was computed as

$$\mathbf{Jf} = \begin{pmatrix} \mathbf{Jf}_{\mathbf{x}_l}(\mathbf{x}_l^n, p_l(t_n)) & \mathbf{Jf}_{p_l}(\mathbf{x}_l^n, p_l(t_n)) \frac{p_l(t_{n+1}) - p_l(t_n)}{h} & f(\mathbf{x}_l^n, p_l(t_n)) \\ 0 & 0 & 1 \\ 0 & 0 & 0 \end{pmatrix} \quad (1)$$

where $\mathbf{Jf}_{\mathbf{x}_l}$ and \mathbf{Jf}_{p_l} indicate Jacobian operators of the function f concerning each of its components and $l = e_p, i, e_s$.

- The full expression for the Jacobian after included the algebraic derivation performed with the MATLAB Symbolic Toolbox is given by

$$\mathbf{Jf} = \begin{pmatrix} 0 & 1 & 0 & x \\ -v_l^2 & -2v_l & H_l v_l p_{l \text{ diff}} + H_l v_l z_{l \text{ diff}} dS(z_l(t)) & H_l v_l (p_l + S(z_l(t))) - v_l^2 y - 2v_l x \\ 0 & 0 & 0 & 1 \\ 0 & 0 & 0 & 0 \end{pmatrix} \quad (2)$$

- Numerical matrices with the pstsynaptic potential constants for each layer $l = e_p, i, e_s$

$$\mathbf{A}_l = \begin{bmatrix} e^{-v_l h} (v_l h + 1) - 1 & e^{-v_l h} h \\ -v_l^2 e^{-v_l h} & e^{-v_l h} (1 - v_l h) - 1 \end{bmatrix} \quad (3)$$

$$\mathbf{B}_l = \begin{bmatrix} \frac{H_l e^{-v_l h} (-v_l h + e^{-v_l h} - 1)}{v_l} & \frac{H_l e^{-v_l h} (v_l h + e^{-v_l h} (v_l h - 2) + 2)}{v_l^2 h} \\ v_l H_l e^{-H_l h} h & \frac{H_l e^{-v_l h} (-v_l h + e^{v_l h} - 1)}{v_l h} \end{bmatrix} \quad (4)$$

$$\mathbf{E}_{l,t} = \begin{bmatrix} p_l(t) + S(z_l(t)) \\ p_{l \text{ diff}}(t) + z_{l \text{ diff}}(t) dS(z_l(t)) \end{bmatrix} \quad (5)$$

The terms $p_{l \text{ diff}}(t)$ and $z_{l \text{ diff}}(t)$ in the $\mathbf{E}_{l,t}$ matrix, represent the difference between the values of $p_l(t)$ and $z_l(t)$ in the current and the next step respectively.

- Following the same analysis was computed the matrix $\mathbf{E}_{u,t}$ for population level

$$\mathbf{E}_{u,t} = \begin{bmatrix} p_u(t) + S(z_u(t)) \\ p_{u \text{ diff}}(t) + z_{u \text{ diff}}(t) dS(z_u(t)) \end{bmatrix} \quad (6)$$

here, the random term $p_u(t)$ in this case constitutes an extension concerning the previous one in terms of dimensionalities. $p_{u \text{ diff}}(t)$ and $z_{u \text{ diff}}(t)$ are the difference between the current and the next step of the values $p_u(t)$ and $z_u(t)$ respectively, with $u = 1, \dots, Nu$.

To determine these expressions for the system level is just needed to specify the frequency band for each population.